

Crystallization Behavior of α -Cellulose Short-Fiber Reinforced Poly(lactic acid) Composites

Jyh-Hong Wu,¹ M. C. Kuo,² Chien-Wen Chen,² Chen-Wei Chen,² Ping-Hung Kuan,²
 Yu-Jheng Wang,² Shu-Yao Jhang²

¹Nano-Powder and Thin Film Technology Center, Industrial Technology Research Institute, Tainan 70955, Taiwan, Republic of China

²Department of Materials Engineering, Kun Shan University, Tainan 71003, Taiwan, Republic of China

Correspondence to: M. C. Kuo (E-mail: muchen@mail.ksu.edu.tw)

ABSTRACT: The isothermal crystallization behavior of α -cellulose short-fiber reinforced poly(lactic acid) composites (PLA/ α -cellulose) was examined using a differential scanning calorimeter and a petrographic microscope. Incorporating a natural micro-sized cellulose filler increased the spherulite growth rate of the PLA from 3.35 $\mu\text{m}/\text{min}$ for neat PLA at 105°C to a maximum of 5.52 $\mu\text{m}/\text{min}$ for the 4 wt % PLA/ α -cellulose composite at 105°C. In addition, the inclusion of α -cellulose significantly increased the crystallinities of the PLA/ α -cellulose composites. The crystallinities for the PLA/ α -cellulose composites that crystallized at 125°C were 48–58%, higher than that of the neat PLA for \sim 13.5–37.2%. The Avrami exponent n values for the neat and PLA/ α -cellulose composites ranged from 2.50 to 2.81 and from 2.45 to 3.44, respectively, and the crystallization rates K of the PLA/ α -cellulose composites were higher than those of the neat PLA. The activation energies of crystallization for the PLA/ α -cellulose composites were higher than that of the neat PLA. The inclusion of α -cellulose imparted more nucleating sites to the PLA polymer. Therefore, it was necessary to release additional energy and initiate molecular deposition. © 2013 Wiley Periodicals, Inc. *J. Appl. Polym. Sci.* 129: 3007–3018, 2013

KEYWORDS: biodegradable; crystallization; differential scanning calorimetry

Received 15 August 2012; accepted 17 January 2013; published online 15 February 2013

DOI: 10.1002/app.39029

INTRODUCTION

Poly(lactic acid) (PLA) is a biodegradable thermoplastic that is inherently brittle. Many methods have been used to improve the brittleness of PLA, including plasticization^{1–5} and copolymerization.^{6,7} Furthermore, natural cellulosic fillers, such as rayon monofilaments, jute bundle fibers,⁸ cellulose nanofibers (CNFs),⁹ and cellulose nanocrystals (CNCs),¹⁰ have been proposed to toughen PLA. In our previous study, we used α -cellulose short fibers to improve the brittleness of PLA polymer.¹¹ Jaskiewicz and Bledzki used rayon monofilaments and jute fibers at 30 wt % to increase the notch impact strength of PLA from \sim 2.4 kJ/m² for neat PLA to 7.5 and 3.5 kJ/m² for PLA/rayon and PLA/jute composites, respectively.⁸ Contrast to the method used by Jaskiewicz and Bledzki, PLA/ α -cellulose composites with low filler content (4 wt %) can improve the toughness of PLA to as much as 6.42 kJ/m², maintaining the intrinsic transparency of PLA.¹¹

Many studies have examined the crystallization behavior of poly(L-lactide) (PLLA) under isothermal crystallization conditions.^{12–15} Yasuniwa et al. investigated the crystallization

behavior of PLLA and proposed that the crystal structures for PLLA isothermally crystallized at temperatures above and below the crystallization temperature (T_c) of PLLA were orthorhombic (α -form) and trigonal (β -form), respectively.¹⁵ Bouapao et al. studied the effects of incorporated amorphous poly(DL-lactide) (PDLLA) on the isothermal crystallization and spherulite growth of crystalline PLLA, and using differential scanning calorimeter (DSC), determined that the crystallinity of neat PLLA is of 59.7%.¹⁶ Furthermore, they indicated that PLLA is crystallizable in the presence of PDLLA at an X_{PDLLA} of 0.3–1, and suggested that the incorporation of PDLLA does not influence the crystalline thickness of PLLA. Ho et al. characterized the molten morphologies following the isothermal crystallization of poly(L-lactide-*block*-dimethyl siloxane-*block*-L-lactide) triblock copolymers, proposing that the crystallization rate of triblock copolymers is less than that of PLLA homopolymer.¹⁷ Eguiburu et al. studied amorphous and crystalline poly(lactides) [poly(D-lactide) (PDLA) and PLLA] blended with poly(methyl methacrylate) (PMMA) and poly(methyl acrylate), concluding that PMMA prevents the crystallization of PLLA and that the PLLA contents in the blend must be higher than 80% to observe the

crystallization and melting of the PLLA crystals during the second-heating run.¹⁸

As mentioned, many natural cellulosic fillers have been proposed to toughen PLA. However, to date, there have been few studies on the crystallization behavior of cellulosic-filler reinforced PLA composites. Qiu and Pan investigated the preparation, crystallization, and hydrolytic degradation of PLLA/polyhedral oligomeric silsesquioxanes (POSS) nanocomposites, determining that the presence of POSS significantly enhances the crystallization rate, improves mechanical properties, and accelerates the hydrolytic degradation of PLLA in the nanocomposites with respect to neat PLLA.¹⁹ Pei et al. studied the crystallization and mechanical properties of cellulose nanocrystal-filled PLLA nanocomposites, and found that the crystallinities for neat PLLA, 2 wt % PLLA/CNC, and 2 wt % PLLA/SCNC (silylation of cellulose nanocrystals) nanocomposites were 14.3, 15.0, and 20.7%, respectively. However, the crystallization rates for the PLLA/CNC and PLLA/SCNC were slightly less than that of the neat PLLA.²⁰

Unlike the blending methods, copolymerization strategies, and filament fiber inclusion, the α -cellulose short fibers may offer an alternate technique to substantially toughen PLA. The α -cellulose is natural and has an abundance of pulps. Unlike the CNF⁹ or CNC,¹⁰ it is easy to obtain and can be used directly without any purification or refinement. PLA/ α -cellulose composites have been successfully fabricated. The microscale filler of α -cellulose can significantly improve the toughness of PLA through fiber pullout and by increasing the microcrack length in the PLA matrix during a fracture. In our previous study, the mechanical properties of the PLA/ α -cellulose composites were characterized and estimated. Because there have been few studies on the crystallization behavior of PLA composites, it is crucial to explore the crystallization behavior of PLA/ α -cellulose and to elucidate the correlation between the mechanical properties and crystallization behavior of PLA/ α -cellulose.

EXPERIMENTAL

Materials

PLA (NatureWorks 4032D) was purchased from Cargill-Dow LLC, and it contains 92% L-lactide and 8% meso-lactide. The molecular weight and density of PLA are 1.8×10^5 – 2.0×10^5 g/mol and 1.25 g/cm³, respectively. The α -cellulose with 200–600 μm in length and 3–50 μm in diameter was purchased from Sigma.

Fabrication of PLA/ α -Cellulose Composites

The fabrication method is the same as our previous work.¹¹ PLA/ α -cellulose composites were fabricated by mixing PLA with α -cellulose fibers using a twin-screw extruder (Nanking Jia-Ya SHJ-20, China) with L/D ratio of 28. The barrel temperatures were 182–190°C, and the screw speed is 20 rpm. Accordingly, the duration of PLA melt in the extruder is about 1 min. The short fibers content were designated as 0, 0.5, 1.0, 2.0, 4.0, 6.0, and 8.0 wt %. The PLA was dried at 80°C for 12 h to remove the moisture. The as-received α -cellulose was dried at 50°C for 12 h before use.

DSC Measurement

A TA DSC (TA Q2000) was applied to investigate the isothermal crystallization behaviors of neat PLA and PLA/ α -cellulose composites. The sample was heated up to 200°C at a rate of 10°C/min under nitrogen atmosphere. At 200°C, this sample was held for 5 min to remove the previous thermal history, and then it was quenched to the predetermined temperatures (95, 100, 105, 110, 115, 120, and 125°C) to undergo isothermal crystallization process. After the isothermal crystallization process, the sample was subsequently heated to 185°C to conduct the second-heating run and to estimate the melting temperature (T_m).

POM Observations

A Zeiss Axioskop 40A petrographic microscope (POM) was used to observe the spherulite morphologies of neat PLA and PLA/ α -cellulose composites under isothermal crystallization. A thin piece of sample was sandwiched between two glass coverslips and placed on a digital hot-stage under nitrogen atmosphere. The hot-stage was rapidly heated to 200°C at 20°C/min and held for 5 min to erase the thermal history of specimens. Then, the neat PLA or PLA/ α -cellulose melt was quenched using liquid nitrogen to the predetermined crystallization temperatures and kept at these temperatures to observe spherulite morphology and to determine the spherulite growth rate of the PLA or PLA/ α -cellulose composite.

RESULTS AND DISCUSSION

PLA Spherulites Growth

This study used POM to determine the spherulite morphologies and growth rates of the neat PLA and PLA/ α -cellulose composites that isothermally crystallized at predetermined temperatures (95, 100, 105, 110, 115, 120, and 125°C), as shown in Figure 1 and Table I. The error on the spherulite dimension of PLA during measurement is about 2–3 μm . The spherulite dimensions for the neat PLA crystallized at 120°C for 8 min reached as high as 79 μm , and adding α -cellulose decreased the spherulite dimension of the PLA matrix. When the cellulose content was 8.0 wt %, the spherulite dimension was 44 μm , a decrease of ~44% compared to that of the neat PLA at 120°C. The inclusion of α -cellulose provided more additional crystallization sites for the PLA molecules to deposit and crystallize, consequently lowering the spherulite dimension of the PLA matrix. Regarding the effects of α -cellulose on the growth rate of the PLA matrix (Table I), the growth rate of the PLA spherulites increased when the natural micro-sized cellulose filler was incorporated, and the highest value of spherulite growth rate occurred with the 4.0 wt % α -cellulose content. The increased growth rate of the PLA spherulites may have been related to heterogeneous nucleation in the PLA/ α -cellulose composites. Furthermore, the α -cellulose in the PLA matrix became aggregated when the α -cellulose content was higher than 4.0 wt %, as shown in Figure 2. This aggregation may explain why the maximum growth rate occurred at 4.0 wt % α -cellulose content. Conversely, the growth rate of the spherulites decreased when the α -cellulose content was higher than 4.0 wt %, suggesting that the mobility hindrance that was increased by the high α -cellulose content dominated the effects of heterogeneous nucleation.

Irrespective of the neat PLA and PLA/ α -cellulose composites, all of the PLA spherulites had their fastest growth rate at a

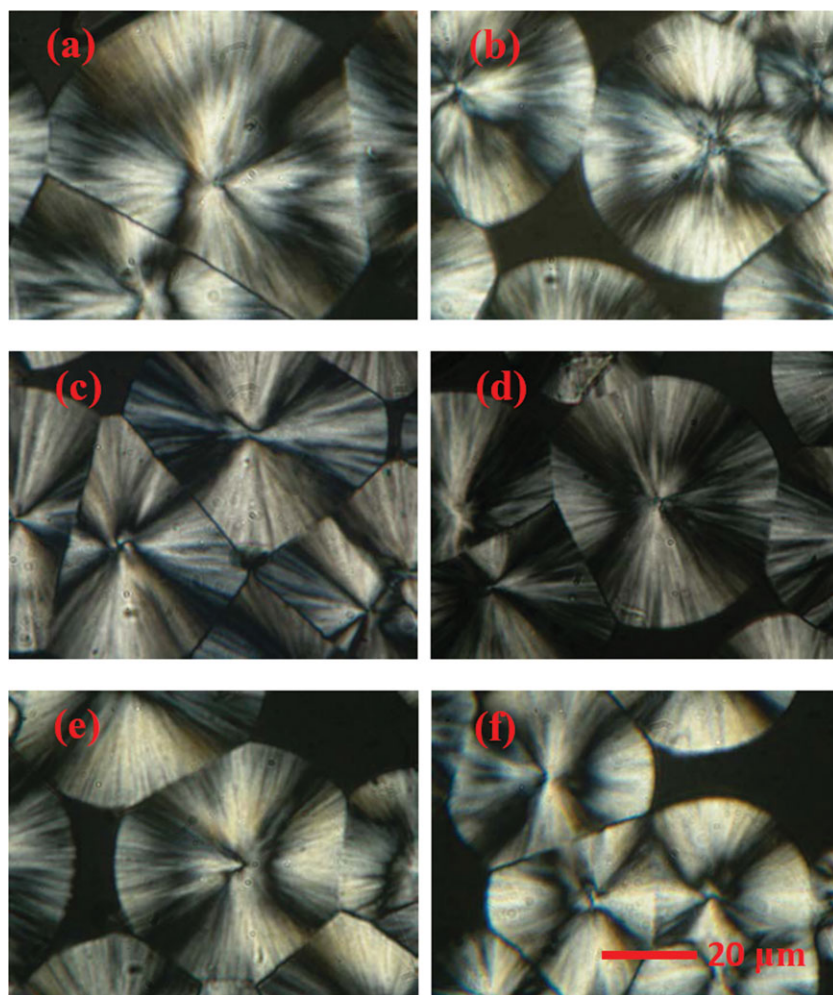


Figure 1. The spherulite dimensions of the neat PLA and PLA/ α -cellulose composites at 120°C for 8 min. The spherulite dimensions for (a) neat, (b) 1.0, (c) 2.0, (d) 4.0, (e) 6.0, and (f) 8.0 wt % were \sim 80, 61, 57, 48, 47, and 44 μm , respectively. [Color figure can be viewed in the online issue, which is available at wileyonlinelibrary.com.]

crystallization temperature of 105°C, indicating that the propagation of the PLA spherulites reached the equilibrium of kinetics and thermodynamics at this temperature.²¹ At 105°C, the growth rate for the 4.0 wt % PLA/ α -cellulose was 5.52 $\mu\text{m}/\text{min}$, higher than that of the neat PLA by \sim 65%. Bouapao et al. proposed that the spherulite growth rates at 105°C for neat PLLA and the PLLA/PDLA (70/30) blend are \sim 4.5 and 3.5 $\mu\text{m}/\text{min}$, respectively.¹⁶ PLA has stereoisomer, such as PLLA, PDLA, and poly(DL-lactide) (PDLLA), where PLLA and PDLA are crystalline and PDLLA is amorphous.¹⁶ In this study, the growth rate for neat PLA was 3.35 $\mu\text{m}/\text{min}$, slightly lower than that of PLLA/PDLA blend (3.5 $\mu\text{m}/\text{min}$). However, the growth rate for 4.0 wt % PLA/ α -cellulose was 5.52 $\mu\text{m}/\text{min}$, higher than that of the PLLA (4.5 $\mu\text{m}/\text{min}$), and the heterogeneous nucleation occurred in the 4.0 wt % PLA/ α -cellulose composites may be responsible for this faster growth rate (5.52 $\mu\text{m}/\text{min}$).

Isothermal Crystallization Behavior of PLA/ α -Cellulose Composites

The isothermal crystallization of the neat PLA and PLA/ α -cellulose composites was performed using DSC at predetermined

temperatures of 95, 100, 105, 110, 115, 120, and 125°C for 60 min. Figure 3 shows the melt-crystallization DSC traces, and Figure 4 shows the selected second-heating DSC traces. As shown in Figure 3, the crystallization enthalpies (ΔH_c) and peak crystallization times (τ_p) of the neat PLA and its composites were determined. In addition, the absolute crystallinities of the neat PLA and its composites can be estimated by using the heat of fusion of an infinitely thick PET crystal, ΔH_f° :^{22,23}

$$X_c = \frac{\Delta H_c}{\Delta H_f^\circ W_{\text{polymer}}} \times 100, \quad (1)$$

where ΔH_f° is \sim 93.7 J/g,²⁴ and W_{polymer} is the weight fraction of the polymer matrix. Furthermore, the melting temperatures of the neat PLA and its composites were measured, as shown in Figure 4. These crystallization parameters are shown in Table II. To possibly eliminate the deviation from DSC sample with different domain sizes, the crystallization parameters for each specimen in Table II were evaluated from three to four times of DSC measurement.

Table I. The Spherulite Growth Rates of the Neat PLA and PLA/ α -Cellulose Composites

Sample	Crystallization temperature (°C)	Growth rate ^a ($\mu\text{m}/\text{min}$)
Neat PLA	95	1.13
	100	2.50
	105	3.35
	110	3.09
	115	2.92
	120	2.49
	125	2.27
α -Cellulose 1.0 wt %	95	1.62
	100	2.72
	105	4.44
	110	4.26
	115	4.01
	120	3.63
	125	3.45
α -Cellulose 2.0 wt %	95	2.28
	100	3.01
	105	4.88
	110	4.69
	115	4.55
	120	4.04
	125	3.74
α -Cellulose 4.0 wt %	95	2.51
	100	3.25
	105	5.52
	110	5.06
	115	4.65
	120	4.14
	125	4.01
α -Cellulose 6.0 wt %	95	1.59
	100	2.24
	105	4.46
	110	4.31
	115	4.01
	120	3.42
	125	3.30
α -Cellulose 8.0 wt %	95	1.46
	100	2.00
	105	3.51
	110	3.40
	115	3.13
	120	3.01
	125	2.63

^aStandard deviation $\pm 0.4 \mu\text{m}/\text{min}$.

As shown in Table II, the inclusion of α -cellulose significantly increased the crystallinities of the PLA/ α -cellulose composites. The crystallinities for the PLA/ α -cellulose composites crystal-

lized at 125°C were 48–58%, higher than that of neat PLA for about 13.5–37.2%. The X_c values for the PLA/ α -cellulose composites increased from 1.0 wt % and reached a maximum value (58.44%) at 4.0 wt %, and decreased when the α -cellulose content was higher than 4.0 wt %. The highest X_c value for the 4.0 wt % α -cellulose content was, to some extent, coupled with the maximum growth rate of the spherulites at this particular α -cellulose content, suggesting that the inclusion of α -cellulose into the PLA matrix increased the crystallization sites and possibly caused the PLA molecules to enter crystallization in

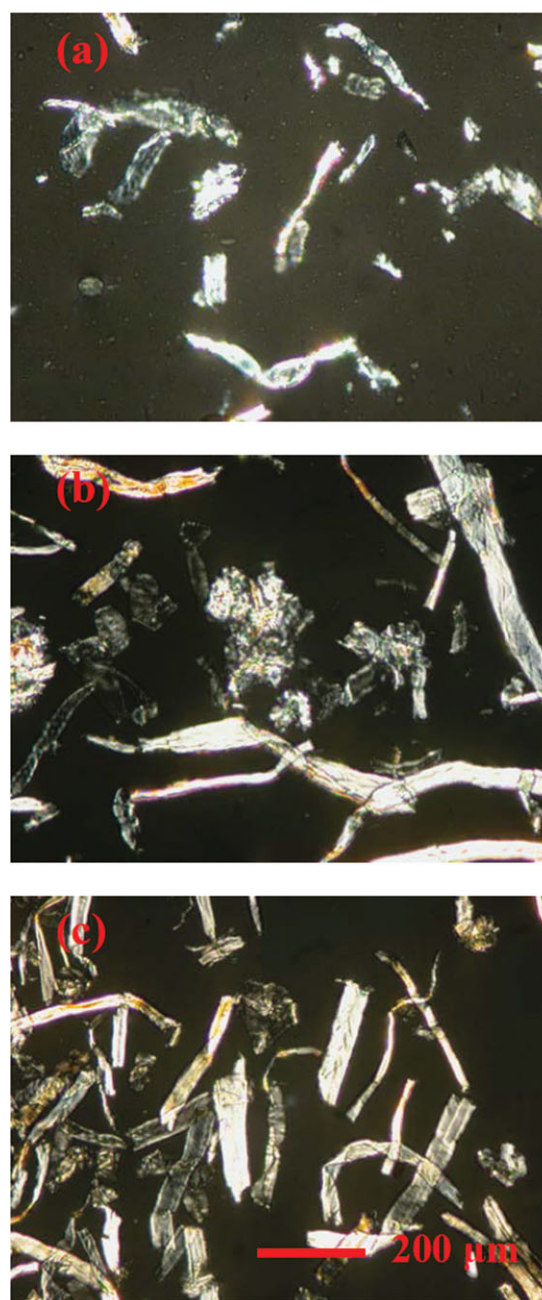


Figure 2. The dispersion of α -cellulose in the PLA matrix. (a), (b), and (c) are the micrographs of the PLA/ α -cellulose composites with α -cellulose contents of 4.0, 6.0, and 8.0 wt %, respectively. [Color figure can be viewed in the online issue, which is available at wileyonlinelibrary.com.]

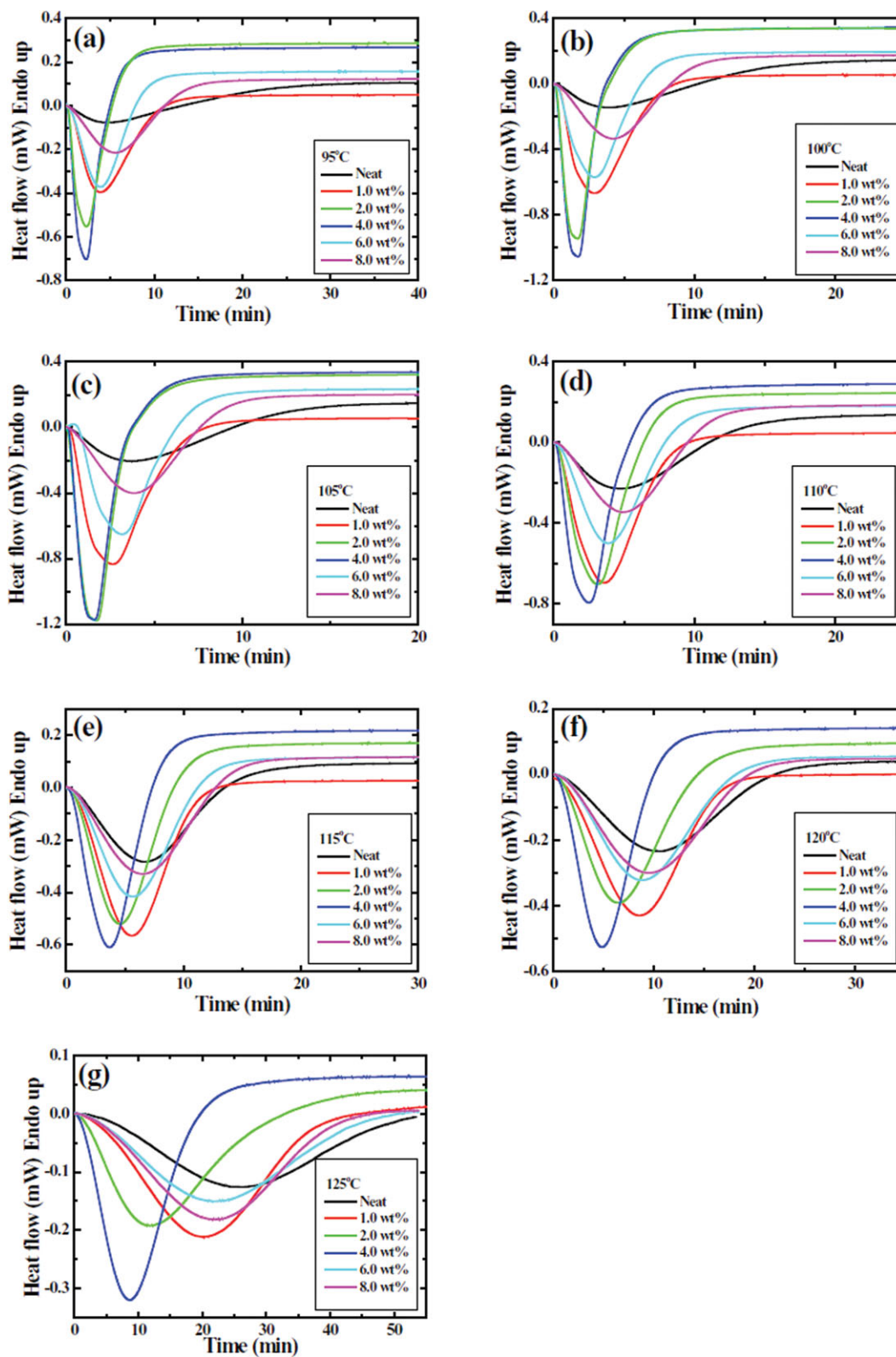


Figure 3. DSC crystallization traces for the neat PLA and PLA/ α -cellulose composites isothermally crystallized at predetermined temperatures. [Color figure can be viewed in the online issue, which is available at wileyonlinelibrary.com.]

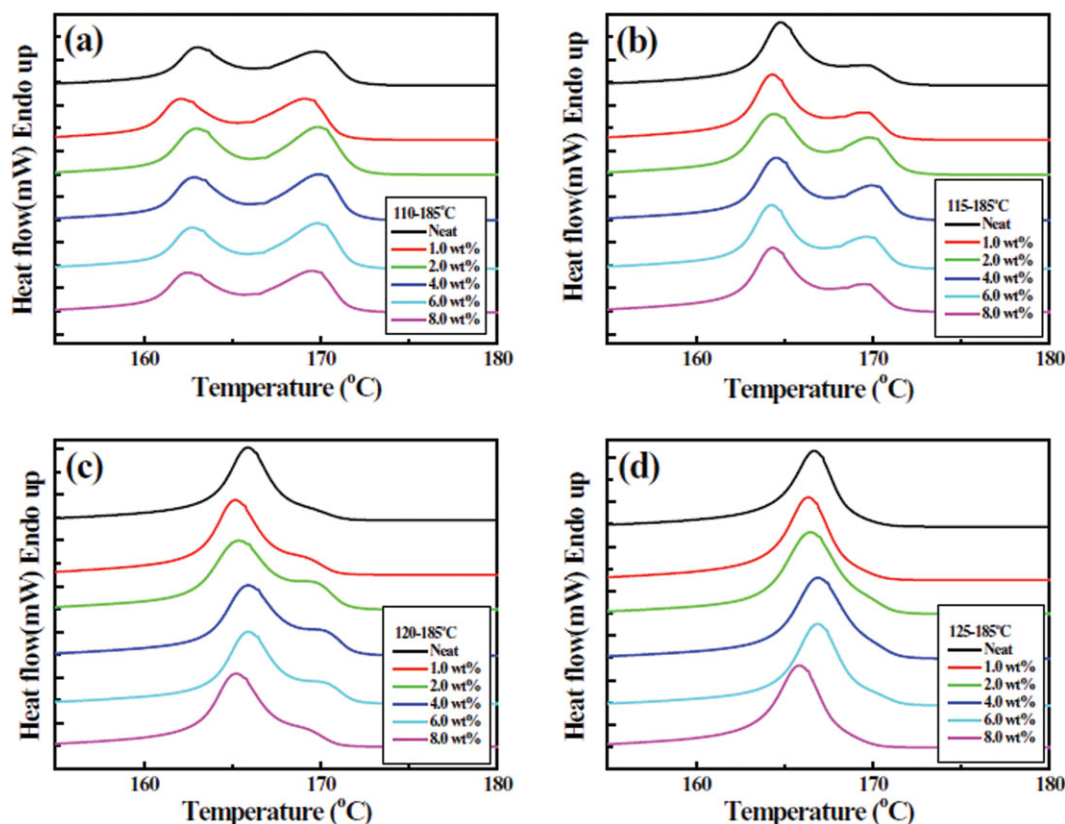


Figure 4. (a), (b), (c), and (d) are the DSC second-heating traces for the neat PLA and PLA/ α -cellulose composites isothermally crystallized at 110, 115, 120, and 125°C, respectively, that were subsequently heated to 185°C to estimate their melting temperatures. [Color figure can be viewed in the online issue, which is available at wileyonlinelibrary.com.]

heterogeneous nucleation. However, the α -cellulose in the PLA matrix aggregated considerably when the α -cellulose content was higher than 4.0 wt % (Figure 2), and this poor dispersion hindered the diffusion of the PLA molecules and suppressed the occurrence of heterogeneous nucleation. However, the PLA composites with cellulose contents higher than 4.0 wt % exhibited substantially higher crystallinity than did neat PLA, explaining why the crystallization sites on the fiber surfaces were still available under high filler contents of 6.0 and 8.0 wt %.

This study used peak crystallization time (τ_p) to define the time from onset to a point where the exothermic peak appeared under isothermal crystallization. If the DSC crystallization trace was symmetric, the peak crystallization time was equal to the crystallization half-life.²⁵ As shown in Table II, the τ_p values for the PLA/ α -cellulose composites decreased from 1.0 wt % PLA/ α -cellulose, and reached a minimum at 4.0 wt % PLA/ α -cellulose, and gradually increased to 6.0 and 8.0 wt % in the PLA/ α -cellulose composites. The inclusion of α -cellulose considerably reduced the τ_p value when the filler content was less than 4.0 wt % compared to the neat PLA. The inclusion of α -cellulose raised the spherulite growth rate and crystallinity of the PLA matrix, but reduced peak crystallization time. Consequently, the cellulose fibers may have induced heterogeneous nucleation. Conversely, the τ_p values of the 8.0 wt % PLA/ α -cellulose composite at lower crystallization temperatures

(95–110°C) were higher than those of neat PLA, indicating that a high α -cellulose content (e.g., 8.0 wt %) may increase the diffusion difficulty of PLA molecules at lower crystallization temperatures. As mentioned, the α -cellulose in the PLA matrix became aggregated when the α -cellulose content was higher than 4.0 wt %, as shown in Figure 2. The aggregation of the α -cellulose simultaneously reduced the spherulite growth rate and crystallinity and increased the crystallization time, and consequently, had an opposite effect on heterogeneous nucleation.

Figure 4 shows the selected second-heating DSC traces for the neat PLA and PLA/ α -cellulose composites, and the corresponding melting temperatures (including lower melting temperature T_{m1} and higher melting temperature T_{m2}) are shown in Table II. The differences among the neat PLA and PLA/ α -cellulose composites in T_{m1} or T_{m2} were minor. The PLA/ α -cellulose composite with a 4.0 wt % α -cellulose content exhibited the highest values in T_{m1} and T_{m2} compared to those of the neat PLA and other PLA/ α -cellulose composites. Conversely, the PLA/ α -cellulose composite with 1.0 wt % α -cellulose content exhibited the lowest values in T_{m1} and T_{m2} . The inclusion of micro-sized α -cellulose greatly increased the crystallinity and reduced crystallization time. Inorganic or organic filler can affect the crystallization behavior of polymer molecules in two manners: (1) It increases the crystallinity and melting temperature through heterogeneous nucleation; or (2) it decreases crystallinity through mobility hindrance. This study showed that the

Table II. The Lower Melting Temperatures (T_{m1}), Higher Melting Temperatures (T_{m2}), Absolute Crystallinities (X_c), and Peak Crystallization Times (τ_p) of the Neat PLA and PLA/ α -Cellulose Composites Isothermally Crystallized at Predetermined Temperatures

Sample	Crystallization temperature (°C)	T_{m1} (°C)	T_{m2} (°C)	X_c (%)	τ_p (min)
Neat PLA	95	150.6	167.9	19.32	4.84
	100	153.3	168.6	22.81	3.89
	105	158.2	169.5	25.44	3.84
	110	163.3	169.7	30.37	4.78
	115	164.8	169.9	36.19	6.73
	120	-	165.9	39.17	10.52
	125	-	166.7	42.60	24.06
α -Cellulose 1.0 wt %	95	150.6	167.1	31.47	3.90
	100	152.9	167.5	35.49	2.87
	105	157.1	168.1	38.99	2.64
	110	162.5	169.3	41.34	3.67
	115	164.0	169.6	41.76	5.64
	120	-	165.2	44.41	8.53
	125	-	166.3	48.33	19.72
α -Cellulose 2.0 wt %	95	150.5	167.8	27.17	2.31
	100	153.0	168.4	30.37	1.76
	105	157.5	169.4	33.30	1.79
	110	162.9	170.0	35.21	3.10
	115	164.7	170.0	40.46	4.50
	120	-	165.4	47.07	7.37
	125	-	166.5	53.84	11.73
α -Cellulose 4.0 wt %	95	150.7	168.0	32.83	2.27
	100	153.2	168.4	39.60	1.69
	105	157.4	169.2	43.90	1.55
	110	162.9	170.1	44.94	2.51
	115	164.5	170.1	45.94	3.66
	120	-	165.9	49.83	4.80
	125	-	166.9	58.44	8.57
α -Cellulose 6.0 wt %	95	150.5	167.8	29.55	3.90
	100	153.0	168.4	35.01	2.90
	105	157.5	169.4	37.83	2.71
	110	162.9	170.0	38.14	3.86
	115	164.7	170.0	41.26	5.64
	120	-	165.9	46.38	8.77
	125	-	166.9	50.97	21.26
α -Cellulose 8.0 wt %	95	150.4	167.5	34.50	5.78
	100	153.0	167.9	37.29	4.27
	105	157.0	168.7	41.52	4.01
	110	162.5	169.6	42.04	4.92
	115	164.0	169.7	42.83	6.54
	120	-	165.2	47.37	9.39
	125	-	165.9	50.91	21.82

inclusion of α -cellulose considerably increased the crystallinity of the PLA matrix, but the difference in the melting temperatures between the neat PLA and its composites polymer was

minor, implying that none of the heterogeneous nucleation or mobility hindrance dominated and that they worked in parallel during isothermal crystallization. At low α -cellulose contents

(1.0–4.0 wt %), α -cellulose was semihomogeneously dispersed in the PLA matrix, as shown in Figure 2. This dispersion favored the PLA/ α -cellulose composites to crystallize in heterogeneous nucleation. However, at high α -cellulose contents (i.e., 6.0 and 8.0 wt %), the aggregation of the α -cellulose considerably increased the mobility hindrance of the PLA segments.

The lowest values of T_{m1} and T_{m2} in the 1.0 wt % PLA/ α -cellulose composite may explain the imperfection of the spherulite morphology. As shown in Figure 2, the inclusion of α -cellulose decreased the dimension of the PLA spherulites compared to the neat PLA. The dimensions of the PLA spherulites decreased continuously from $\sim 80 \mu\text{m}$ for the neat PLA to $44 \mu\text{m}$ for the 8.0 wt % PLA/ α -cellulose composite, suggesting that the α -cellulose increased the crystallization sites but hindered the molecule diffusion of the PLA during crystallization. At low α -cellulose content (e.g., 1 wt %), the effect of heterogeneous nucleation may not exceed the effect of mobility hindrance. However, the predominance of mobility hindrance could cause imperfections in the spherulites or lower the values in T_{m1} and T_{m2} . However, heterogeneous nucleation became predominant when the α -cellulose content was greater than 1 wt %. As shown in Figure 4 and Table II, all of the neat PLA and PLA/ α -cellulose composites exhibited double melting behavior when the predetermined temperatures ranged from 95 to 115°C. T_{m1} is an unstable melting temperature and can easily be affected by annealing conditions. The inclusion of α -cellulose did not alter the double melting behavior of the PLA, indicating that the inclusion of α -cellulose did not change the crystal structure of the PLA. Pan et al. suggested that the transition from the α' to the α form occurs at a T_c of 110–120°C.²⁶ This study followed the Pans' study.

The crystallization behavior of the PLA/ α -cellulose composites may reflect the mechanical properties of these composites. In our previous study, the ultimate tensile strength (UTS) and Young's modulus (E) of the PLA/ α -cellulose composites decreased at filler contents of 0.5 and 1.0 wt %, but improved when the filler contents increased.¹¹ Furthermore, the elongation at break (ϵ_b) and notched impact strength of the PLA/ α -cellulose composites were considerably improved compared to the neat PLA. The decreases in the spherulite dimensions (Figure 1) and melting temperatures (Table II) may account for the reduced UTS and E at the filler contents of 0.5 and 1.0 wt %. Conversely, the smaller crystallites in the PLA/ α -cellulose composites may have induced grain boundary sliding, increasing the elongation at the break and improving the impact strength of the PLA/ α -cellulose composites. Smaller PLA spherulites can have more defects in the crystallites, reflecting the reduced melting temperatures compared to the neat PLA. This reduction may have caused the decreases in UTS and E of the PLA/ α -cellulose composites at the filler contents of 0.5 and 1.0 wt %. However, the substantially higher values in the crystallinities of the PLA/ α -cellulose composites with α -cellulose contents higher than 1 wt % compensated for the defects and smaller dimensions of the PLA crystallites. Consequently, the incorporation of α -cellulose into the PLA matrix increased the crystallization sites and imparted smaller crystallites and higher crystallinity compared to the neat PLA, improving the impact strength, UTS, and E of the resulting PLA composites.

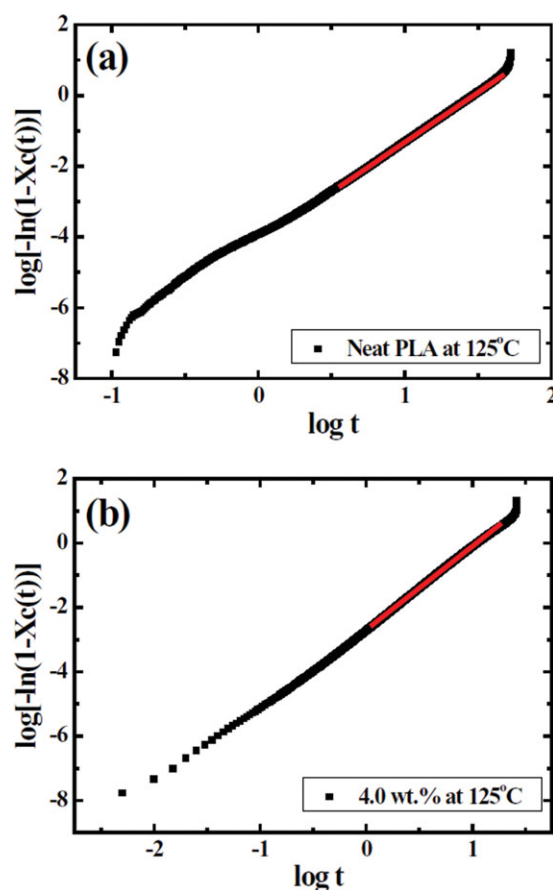


Figure 5. Selected Avrami plots of $\log[-\ln(1 - X_c(t))]$ vs. $\log t$ for (a) neat PLA and (b) PLA/ α -cellulose composite isothermally crystallized at 125°C. [Color figure can be viewed in the online issue, which is available at wileyonlinelibrary.com.]

Isothermal Crystallization Kinetics

The Avrami model can be used to estimate the kinetic parameters under isothermal crystallization, as follows:²¹

$$1 - X_c(t) = \exp(-Kt^n), \quad (2)$$

$$\log[-\ln(1 - X_c(t))] = n \log t + \log K. \quad (3)$$

A plot of $\log[-\ln(1 - X_c(t))]$ versus $\log t$ yields slope n , the Avrami exponent, and the intercept $\log K$, as shown in Figure 5. The parameters of K and n are diagnostics of the crystallization mechanism.²¹ To estimate the Avrami exponents n for the primary crystallization, linear fittings were performed from $\log[-\ln(1 - X_c(t))]$ being -2.0 to 0 , corresponding to X_c equaling 0.01 – 0.63 . Table III shows the kinetics parameters of the neat PLA and PLA/ α -cellulose composites.

The n values for the neat and PLA/ α -cellulose composites at predetermined temperatures ranged from 2.50 to 2.81 and from 2.45 to 3.44, respectively, as shown in Table III. Consequently, the crystals of the neat PLA grew dominantly in a combination of three-dimensional (3D) and two-dimensional (2D) propagation. Conversely, the PLA/ α -cellulose composites had a greater chance to propagate their crystals in a 3D manner, except for

Table III. Isothermal Crystallization Kinetic Parameters of the PLA and PLA/ α -Cellulose Composites at Predetermined Temperatures

Crystallization temperature (°C)	Neat PLA		α -Cellulose 1.0 wt %		α -Cellulose 2.0 wt %		α -Cellulose 4.0 wt %		α -Cellulose 6.0 wt %		α -Cellulose 8.0 wt %	
	<i>n</i>	$K \times 10^3$ (min ^{1/<i>n</i>)}	<i>n</i>	$K \times 10^3$ (min ^{1/<i>n</i>)}	<i>n</i>	$K \times 10^3$ (min ^{1/<i>n</i>)}	<i>n</i>	$K \times 10^3$ (min ^{1/<i>n</i>)}	<i>n</i>	$K \times 10^3$ (min ^{1/<i>n</i>)}	<i>n</i>	$K \times 10^3$ (min ^{1/<i>n</i>)}
95	2.50	17.01	2.59	63.59	2.60	232.26	2.70	460.69	2.58	57.37	2.41	18.58
100	2.52	13.94	2.64	35.04	2.66	203.21	2.74	247.98	2.62	41.43	2.44	15.55
105	2.54	9.75	2.74	17.74	2.78	78.56	2.83	83.52	2.66	17.64	2.47	10.64
110	2.58	7.62	2.88	10.51	3.03	35.36	3.06	78.79	2.69	14.37	2.49	7.16
115	2.60	4.91	2.89	4.97	3.13	10.49	3.22	19.40	2.79	5.93	2.52	5.16
120	2.62	1.54	2.90	1.86	3.30	4.29	3.34	8.69	2.91	1.73	2.57	1.90
125	2.81	0.07	3.25	0.20	3.44	0.68	3.82	2.03	3.02	0.19	2.74	0.15

those with high α -cellulose contents (i.e., 6.0 and 8.0 wt %). The high *n* value for the PLA/ α -cellulose composite ascribed to the following two reasons: (1) the occurrence of heterogeneous nucleation and (2) the PLA/ α -cellulose composites possessed higher crystallinity and spherulite growth rates than did the neat PLA. Therefore, this study proposes that these PLA composites initiated the occurrence of heterogeneous nucleation, resulting in higher *n* values. As shown in Table III, the *n* value increased with increasing α -cellulose content, but decreased when the cellulose content was higher than 4.0 wt %. Finally, the *n* values for the 8.0 wt % PLA/ α -cellulose composite were slightly lower than those of the neat PLA. The mobility hindrance for the 8.0 wt % PLA/ α -cellulose suppressed the occurrence of heterogeneous nucleation and resulted in a reduced *n* value. An additional reason is that the polymer film thickness in the aluminum pan during the DSC measurement was $\sim 100 \mu\text{m}$.²⁷ Therefore, the larger dimension of the spherulites may have caused the lower *n* value during the last stage of isothermal crystallization. As shown Figure 1, the spherulite dimensions (120°C for 8 min) were 80 and 60–44 μm for the neat PLA and PLA/ α -cellulose composites, respectively. Therefore, it is proposed that PLA/ α -cellulose composites with smaller spherulite dimensions compared to neat PLA exhibit higher *n* values. For the PLA composites with low α -cellulose contents (e.g., 1.0–4.0 wt %), the occurrence of heterogeneous nucleation was predominant, meaning that they had higher *n* values than did of the neat PLA. However, the PLA composites with high α -cellulose contents (e.g., 6.0 and 8.0 wt %) were associated with lower *n* values because of the predominance of the mobility hindrance.

Regarding the effect of α -cellulose on the crystallization rate *K* (Table III), the inclusion of α -cellulose significantly increased the crystallization rates of the PLA/ α -cellulose composites even for the 8.0 wt % PLA/ α -cellulose, compared to the neat PLA. As expected, the α -cellulose in the PLA matrix increased the crystallization sites in which the PLA molecules could be deposited. As the same event happened on the Avrami exponent *n* of the PLA/ α -cellulose composites, the *K* value increased with increasing α -cellulose content but decreased when the cellulose content was greater than 4.0 wt %.

Activation Energy of Isothermal Crystallization

According to the Arrhenius model, the crystallization rate parameter *K* can be approximately described by the following equation:²⁸

$$K^{1/n} = k_0 \exp(-\Delta E/RT_c), \quad (4)$$

$$\frac{1}{n} \ln K = \ln k_0 - \frac{\Delta E}{RT_c}, \quad (5)$$

where *k*₀ is a temperature-independent pre-exponential factor, and *R* is the universal gas constant, and (− ΔE) is the activation energy for isothermal crystallization. A plot of (1/*n*) ln *K* versus 1/*T*_c obtains the activation energy for the primary crystallization stage, as shown in Figure 6.

The values of (− ΔE) for the neat PLA, 1.0, 2.0, 4.0, 6.0, and 8.0 wt % PLA/ α -cellulose composites were 41.1, 52.2, 63.3, 63.5, 54.0, and 45.5 kJ/mol, respectively. The inclusion of α -cellulose into the PLA imparted additional nucleating sites to the

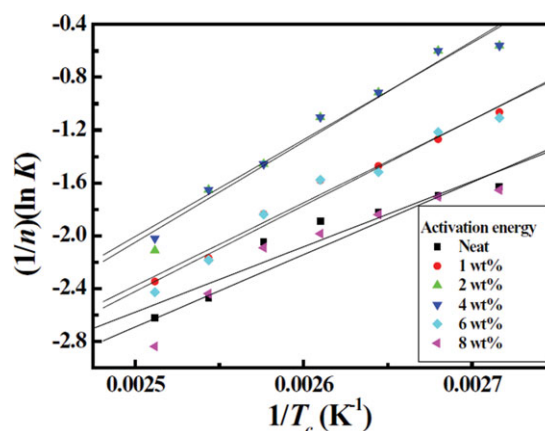


Figure 6. Activation energies estimated from the linear fits (black lines) for the neat PLA and PLA/ α -cellulose under isothermal crystallization. The values of (− ΔE) for the neat PLA, 1.0, 2.0, 4.0, 6.0, and 8.0 wt % PLA/ α -cellulose composites were 41.1, 52.2, 63.3, 63.5, 54.0, and 45.5 kJ/mol, respectively. [Color figure can be viewed in the online issue, which is available at wileyonlinelibrary.com.]

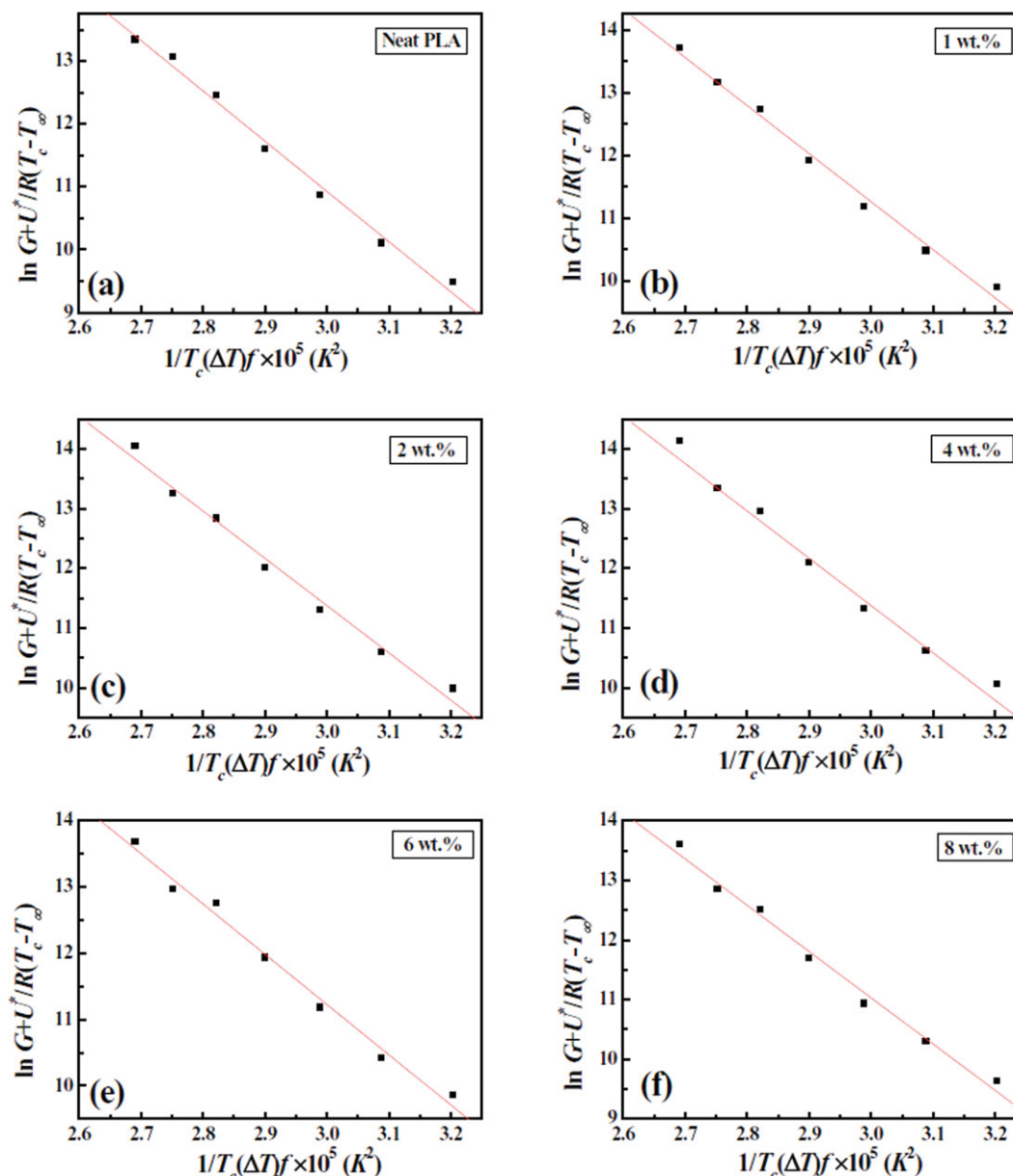


Figure 7. The Lauritzen-Hoffman plots for the neat PLA and PLA/ α -cellulose on the estimation of nucleation parameter K_g . The K_g values for the neat PLA, 1.0, 2.0, 4.0, 6.0, and 8.0 wt % PLA/ α -cellulose composites were 6.00×10^5 , 5.66×10^5 , 5.59×10^5 , 5.05×10^5 , 5.76×10^5 , and 5.94×10^5 K², respectively. [Color figure can be viewed in the online issue, which is available at wileyonlinelibrary.com.]

polymer. Consequently, it was necessary to release additional energy and to initiate molecular depositions. The lowest value of 41.1 J/mol for the neat PLA reflected the smallest number of nucleating sites that could be obtained during the nucleation period. The crystallization process was exothermic, and the fewer nucleating sites resulted in reduced activation energy. The PLA/ α -cellulose composite with 4.0 wt % α -cellulose content had the highest activation energy, suggesting that occurrence of heterogeneous nucleation in this composite was easier than in the neat PLA and the other composites.

Nucleation Parameters of the Isothermal Crystallization

For a better understanding of the crystal growth kinetics of the neat PLA and PLA/ α -cellulose composites that were isothermally

crystallized from melting, a secondary nucleation theory known as Lauritzen-Hoffman equation was used to estimate the spherulitic growth rate G of the neat PLA and its composites.²⁹ The radius growth rate of spherulites, as shown in Table I, can be used to describe the spherulitic growth rate G .³⁰ At a given crystallization temperature T_c , the spherulitic growth rate G can be expressed by the following equation:^{30,31}

$$G = G_0 \exp \left[-\frac{U^*}{R(T_c - T_\infty)} \right] \exp \left[-\frac{K_g}{T_c(\Delta T)f} \right] \quad (6)$$

where G_0 is a pre-exponential factor; U^* is the energy for transporting the polymer chain segments to the crystallization site that is commonly given a universal value of 6280 J/mol; R is the

gas constant; T_∞ is the temperature below which the polymer chain movement ceases and is defined as $(T_g - C)$, where T_g is the glass transition temperature and C is a constant of 30; K_g is a nucleation parameter related to the fold and lateral surface energies; ΔT is the degree of supercooling defined as $T_m^o - T_c$; T_m^o is the equilibrium melting temperature; f is a corrective factor for the decreasing of the enthalpy of fusion using crystallization; and $f = 2T_c(T_c + T_m^o)$. The T_g value from the DSC for the PLA was 57.9°C.¹⁶ The T_m^o value for the PLA was 212°C.³⁰ Equation (6) can be rewritten as follows:

$$\ln G + \frac{U^*}{R(T_c - T_\infty)} = \ln G_0 - \frac{K_g}{T_c(\Delta T)f}. \quad (7)$$

A plot of $\ln G + U^*/R(T_c - T_\infty)$ versus $1/T_c(\Delta T)f$ yielded a slope of $-K_g$, as shown in Figure 7. The K_g values for the neat PLA, 1.0, 2.0, 4.0, 6.0, and 8.0 wt % PLA/ α -cellulose composites were 6.00×10^5 , 5.66×10^5 , 5.59×10^5 , 5.05×10^5 , 5.76×10^5 , and 5.94×10^5 K², respectively. The first exponential term of (6) was related to the temperature dependence of the chain mobility, and was therefore a diffusion consideration. The second exponential term was associated with the nucleation process for regime II in which the normal spherulites were formed. The nucleation constant K_g is proportional to $\Delta \cdot \Delta_e$, where Δ is the fold surface free energy and Δ_e is the lateral surface free energy during the nucleation process.³⁰ The addition of α -cellulose decreased the value of the PLA during the nucleation process, but increased the spherulitic growth rate, as shown in Table I. Weng et al. suggested that the inclusion of 1.5 wt % foliated graphite (FG, 50 nm in thickness) into a nylon 6 matrix would increase the K_g value of nylon 6. In addition, they further proposed that motion in the nylon 6 chains is more difficult to obtain in nanocomposite.³² Our previous study on the crystallization kinetics of PET/PETG/clay showed the same trend as the results obtained by Weng et al.³¹ However, in this study, the addition of α -cellulose decreased the K_g value, although the microfiller and nanofiller may have behaved differently during the nucleation process. The addition of the nanofiller may have substantially increased the motion hindrance of the polymer molecules because they were fewer free spaces to which the molecules could diffuse. Motion hindrance may have dominated the crystallization process. However, the microfiller offered more free spaces than did the nanofiller system, and consequently, the available crystallization sites on the surfaces of the microfillers had a predominant role in crystallization compared to motion hindrance.

CONCLUSIONS

The incorporation of α -cellulose reduced the spherulite dimension of the PLA matrix but increased the spherulite growth rate of the PLA from 3.35 $\mu\text{m}/\text{min}$ for the neat PLA at 105°C to 5.52 $\mu\text{m}/\text{min}$ for the 4 wt % PLA/ α -cellulose composite at 105°C. In addition, the α -cellulose significantly increased the crystallinities of the PLA/ α -cellulose composites. The crystallinities for the PLA/ α -cellulose composites that crystallized at 125°C were 48–58%, higher than that of the neat PLA for ~13.5–37.2%. Furthermore, the inclusion of α -cellulose substantially reduced the τ_p value compared to the neat PLA, suggesting

that the inclusion of α -cellulose induced heterogeneous nucleation. The Avrami exponent n values for the neat and PLA/ α -cellulose composites ranged from 2.50 to 2.81 and from 2.45 to 3.44, respectively. The crystallization rates K of the PLA/ α -cellulose composites were higher than those of the neat PLA, suggesting that the PLA/ α -cellulose composites would have a greater chance to propagate their crystals in a 3-D manner than did the neat PLA. The activation energies of crystallization for the PLA/ α -cellulose composites were all higher than that of the neat PLA. The inclusion of α -cellulose imparted more nucleating sites to the PLA polymer, and it was consequently necessary to release additional energy and to initiate molecular deposition. The K_g values for the neat PLA, 1.0, 2.0, 4.0, 6.0, and 8.0 wt % PLA/ α -cellulose composites were 6.00×10^5 , 5.66×10^5 , 5.59×10^5 , 5.05×10^5 , 5.76×10^5 , and 5.94×10^5 K², respectively. The addition of α -cellulose decreased the K_g value of PLA during the nucleation process and increased the spherulitic growth rate.

REFERENCES

- Labrecque, L. V.; Kumar, R. A.; Dave, V.; Gross, R. A.; McCarthy, S. P. J. *Appl. Polym. Sci.* **1997**, *66*, 1507.
- Ljungberg, N.; Wesslen, B. *Polymer* **2003**, *44*, 7679.
- Jacobsen, S.; Fritz, H. G. *Polym. Eng. Sci.* **1996**, *36*, 2799.
- Hu, Y.; Rogunova, M.; Topolkaraev, V.; Hiltner, A.; Baer, E. *Polymer* **2003**, *44*, 5701.
- Jacobsen, S.; Fritz, H. G. *Polym. Eng. Sci.* **1999**, *39*, 1303.
- Zeng, J. B.; Li, Y. D.; Zhu, Q. Y.; Yang, K. K.; Wang, X. L.; Wang, Y. Z. *Polymer* **2009**, *50*, 1178.
- Ho, C. H.; Jang, G. W.; Lee, Y. D. *Polymer* **2010**, *51*, 1639.
- Bledzki, A. K.; Jazkiewicz, A. *Compos. Sci. Technol.* **2010**, *70*, 1687.
- Jonoobi, M.; Harun, J.; Mathew, A. P.; Oksman, K. *Compos. Sci. Technol.* **2010**, *70*, 1742.
- Pei, A.; Zhou, Q.; Berglund, L. A. *Compos. Sci. Technol.* **2010**, *70*, 815.
- Wu, J. H.; Kuo, M. C.; Chen, C. W.; Hsu, Y. L.; Kuan, P. H.; Lee, K. Y., Submitted to *J. Appl. Polym. Sci.* **2012**.
- Vasanthakumari, R.; Pennings, A. J. *Polymer* **1983**, *24*, 175.
- Miyata, T.; Masuko, T. *Polymer* **1998**, *39*, 5515.
- Iannace, S.; Nicolais, L. J. *Appl. Polym. Sci.* **1997**, *64*, 911.
- Yasuniwa, M.; Tsubakihara, S.; Iura, K.; Ono, Y.; Dan, Y.; Takahashi, K. *Polymer* **2006**, *47*, 7554.
- Bouapao, L.; Tsuji, H.; Tashiro, K.; Zhang, J.; Hanesaka, M. *Polymer* **2009**, *50*, 4007.
- Ho, C. H.; Jang, G. W.; Lee, Y. D. *Polymer* **2010**, *51*, 1639.
- Eguibulu, J. L.; Iruin, J. J.; Fernandez-Berridi, M. J.; San Roman, J. *Polymer* **1998**, *39*, 6891.
- Qiu, Z.; Pan, H. *Compos. Sci. Technol.* **2010**, *70*, 1089.
- Pei, A.; Zhou, Q.; Berglund, L. A. *Compos. Sci. Technol.* **2010**, *70*, 815.

21. Sperling, L. H. *Introduction to Physical Polymer Science*, 2nd ed.; Wiley: Singapore, **1993**.
22. Kim, S. H.; Ahn, S. H.; Hirai, T. *Polymer* **2003**, *44*, 5625.
23. Wu, J. H.; Yen, M. S.; Chen, C. W.; Kuo, M. C.; Tsai, F. K.; Kuo, J. S.; Yang, L. H.; Huang, J. C. J. *Appl. Polym. Sci.* **2012**, *125*, 494.
24. Antoine, L. D.; Peter, D.; Christophe, B. *Compos. Sci. Technol.* **2010**, *70*, 231.
25. Munehisa, Y.; Shinsuke, T.; Koji, I.; Yoshinori, O.; Yusuke, D.; Kazuhisa, T. *Polymer* **2006**, *47*, 7554.
26. Pan, P.; Zhu, B.; Kai, W.; Dong, T.; Inoue, Y. J. *Appl. Polym. Sci.* **2008**, *107*, 54.
27. Chen, M.; Chang, W. C.; Lu, H. Y.; Chen, C. H.; Peng, J. S.; Tsai, C. J. *Polymer* **2007**, *48*, 5408.
28. Liu, S.; Yu, Y. N.; Cui, Y.; Zhang, H. F.; Mo, Z. S. J. *Appl. Polym. Sci.* **1998**, *70*, 2371.
29. Hoffman, J. D.; Miller, R. L.; Marand, H.; Roitman, D. B. *Macromolecules* **1992**, *25*, 2221.
30. Tsuji, H.; Tezuka, Y.; Saha, S. K.; Suzuki, M.; Itsuno, S. *Polymer* **2005**, *46*, 4917.
31. Wu, J. H.; Yen, M. S.; Kuo, M. C.; Wu, C. P.; Leu, M. T.; Li, C. H.; F. K. Tsai, F. K. J. *Appl. Polym. Sci.* **2012**, DOI: 10.1002/APP.38203.
32. Weng, W.; Chen, G.; Wu, D. *Polymer* **2003**, *44*, 8119.